Vibrational spectra and lattice thermal conductivity of kesterite-structured Cu_2ZnSnS_4 and $Cu_2ZnSnSe_4$

Jonathan M. Skelton,[1] Adam J. Jackson,[1] Mirjana Dimitrievska,[2] Suzanne K. Wallace,[1] and Aron Walsh[1,a]
[1]*Centre for Sustainable Chemical Technologies and Department of Chemistry, University of Bath, Claverton Down, Bath BA2 7AY, United Kingdom*
[2]*Catalonia Institute for Energy Research (IREC), Jardins de les Dones de Negre 1, 08930 Sant Adria de Besos, Spain*

(Received 28 February 2015; accepted 26 March 2015; published online 7 April 2015)

Cu_2ZnSnS_4 (CZTS) is a promising material for photovoltaic and thermoelectric applications. Issues with quaternary semiconductors include chemical disorder (e.g., Cu–Zn antisites) and disproportionation into secondary phases (e.g., ZnS and Cu_2SnS_3). To provide a reference for the pure kesterite structure, we report the vibrational spectra—including both infra-red and Raman intensities—from lattice-dynamics calculations using first-principles force constants. Three-phonon interactions are used to estimate phonon lifetimes (spectral linewidths) and thermal conductivity. CZTS exhibits a remarkably low lattice thermal conductivity, competitive with high-performance thermoelectric materials. Transition from the sulfide to selenide ($Cu_2ZnSnSe_4$) results in softening of the phonon modes and an increase in phonon lifetimes. [http://dx.doi.org/10.1063/1.4917044]

The quaternary semiconductor Cu_2ZnSnS_4 (CZTS) has been widely studied as an earth-abundant light-absorbing material for thin-film photovoltaics. The record light-to-electron conversion efficiencies for CZTS and $Cu_2ZnSnSe_4$ (CZTSe) solar cells now exceed 12%.[1,2] A limiting factor is the low open-circuit voltage, at less than half the value of the band gap, which has been associated with electron-hole recombination in the bulk material that may be related to inhomogeneity in the distribution of Cu, Zn, and Sn.[3,4]

The ground-state crystal structure of CZTS is kesterite (space group $I\bar{4}$); the coordination environment of each metal and anion is close to tetrahedral, leading to a conventional unit cell which is analogous to a $1 \times 1 \times 2$ supercell expansion of the zinc-blende structure. Each S is surrounded by two Cu, one Zn, and one Sn, as required by local charge neutrality (or equivalently, the valence-octet rule).[5] This bonding requirement is also satisfied by the stannite structure (space group $I\bar{4}2m$).[6]

For typical material preparation conditions, disorder in the Cu and Zn occupancies is found.[7–9] To further complicate matters, a number of secondary binary and ternary phases can be formed by the same elements, which also adopt tetrahedral structures.[10] Quantification of the degree of chemical disorder and disproportionation is difficult using standard laboratory X-ray diffraction, owing to the similar cross-sections of Cu and Zn, and the structural similarity of CZTS to its competing phases, e.g., ZnS and Cu_2SnS_3.[10] Raman spectroscopy, besides being a widely used tool for structural characterisation,[11–14] may also serve as a powerful technique for better characterization of the disorder effects in kesterites.[15] This is due to the fact that the frequency, shape, and spectral intensity of Raman modes are extremely sensitive to the presence of defects in the material.

In this Letter, we investigate the thermal physics of kesterite-structured CZTS and CZTSe using first-principles lattice-dynamics calculations. We report the phonon vibrational density of states

[a]Electronic mail:a.walsh@bath.ac.uk

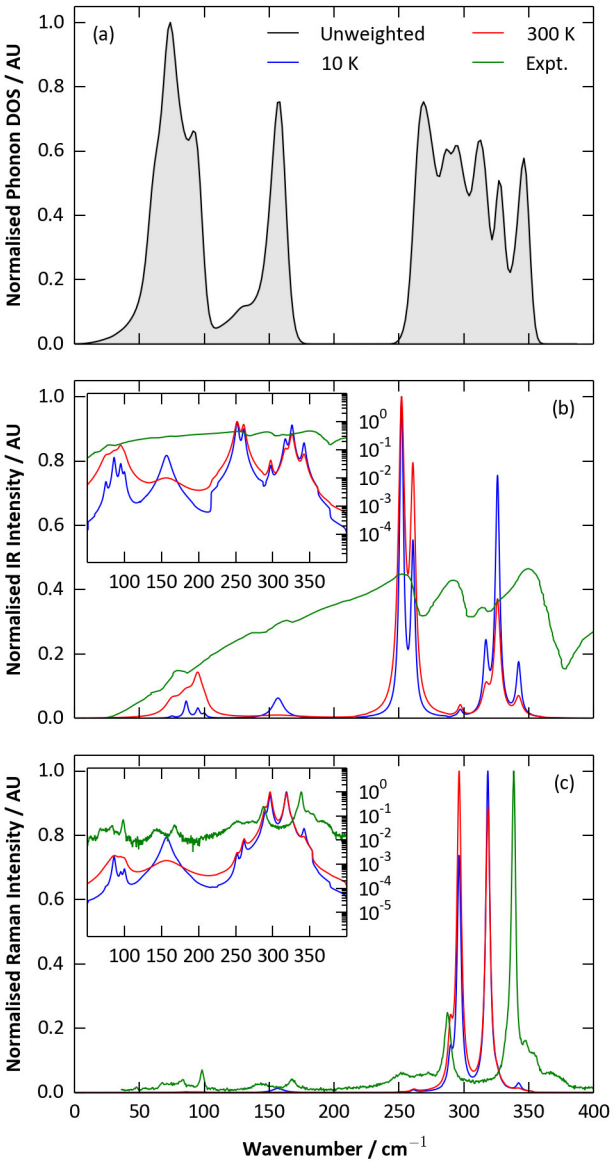

FIG. 1. Calculated phonon density of states (a) and simulated infra-red (b) and Raman (c) spectra of kesterite-structured Cu_2ZnSnS_4. The IR and Raman spectra have been broadened with the calculated 10 K (blue) and 300 K (red) phonon lifetimes. The measured IR spectrum from 1991 (Ref. 24) and Raman spectrum from 2014 (Ref. 14) are overlaid in green. Inset: the IR/Raman spectra on a log scale. Note that LO/TO splitting is not included in these calculated phonon spectra.

(DOS), as well as the simulated Raman and infra-red (IR) spectra. We go beyond the harmonic approximation for vibrations and consider anharmonic three-phonon interactions, allowing us to estimate phonon lifetimes, and hence to predict spectral linewidths and lattice thermal conductivity.

The crystal structures of CZTS and CZTSe were optimised with respect to both internal forces and external pressure using Density Functional Theory (DFT), with the exchange-correlation functional of Perdew, Burke, and Ernzerhof revised for solids (PBEsol).[16] This level of theory provided quantitative agreement with experiment for the phonon dispersions of the lead chalcogenides.[17] Total energy and forces were calculated using the VASP code,[18,19] a 550 eV plane-wave cutoff, and a Γ-centred k-point mesh with $4 \times 4 \times 4$ subdivisions for the primitive unit cell. The projector augmented-wave method[20] including scalar-relativistic effects was employed. Beginning with a CZTS structure from all-electron calculations with the same functional,[21] it was found to be necessary to treat the semi-core Cu $3p$ states, but not the Sn $4d$ states, as valence to converge the total energy and stress

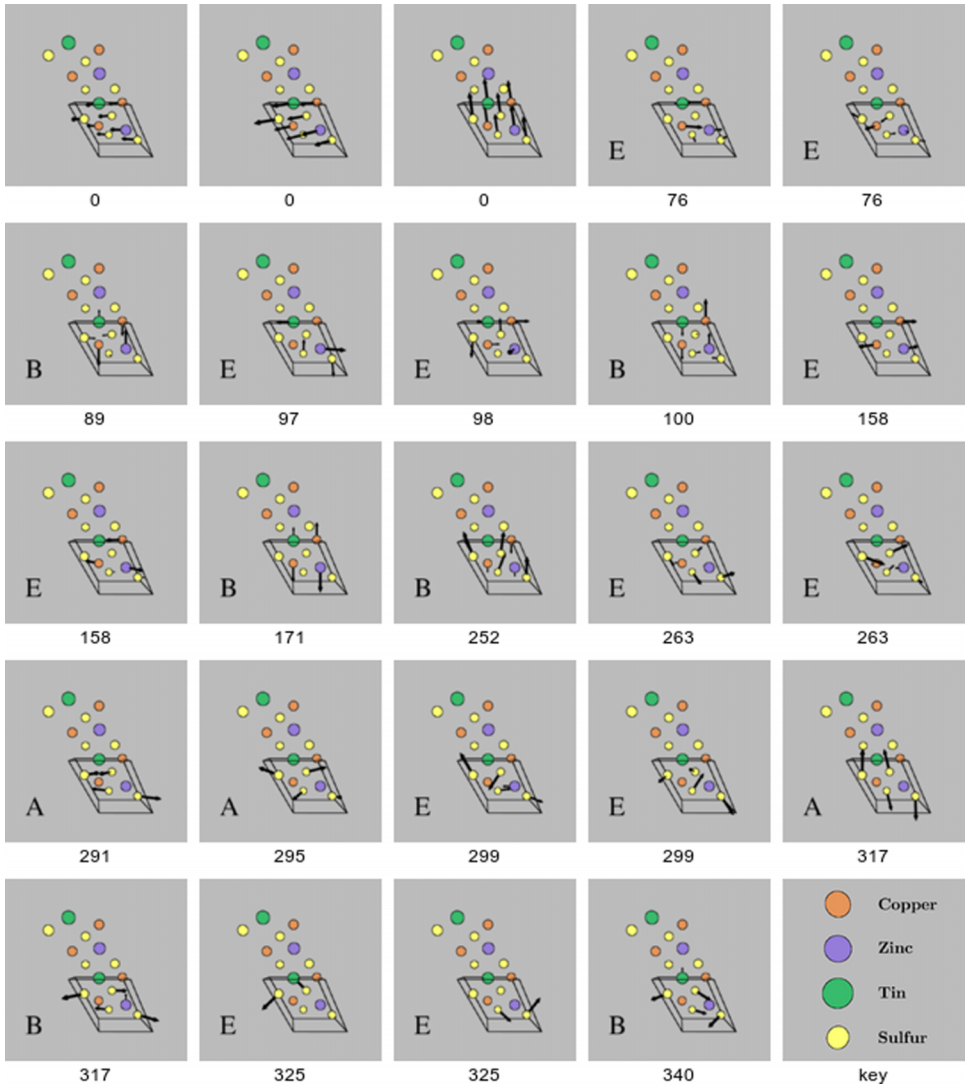

FIG. 2. Eigenvectors of the 24 Γ-point vibrational eigenmodes for Cu_2ZnSnS_4. The upper-case letter gives the irreducible representation (S_4 point group), while the numbers give the mode frequencies in cm^{-1}. Note that the three acoustic modes have zero frequency at the Γ-point. These harmonic modes were computed using FHI-AIMS with the setup previously reported.[21] (Multimedia view) [URL: http://dx.doi.org/10.1063/1.4917044.1]

tensor. Neither of these states are involved in the chemical bonding, but they can influence indirectly the valence electronic structure and hence atomic forces. This treatment was also applied to CZTSe. Internal structural parameters were converged to within 10^{-7} eV or until the magnitude of the forces on the ions was less than 10^{-3} eV/Å.

The Phonopy package was used for lattice dynamics, including structure generation and post-processing using the direct (supercell) approach.[22] The extension of the finite-displacement method to three-phonon interactions and thermal conductivity (solution of the Boltzmann transport equation within the relaxation time approximation) was recently reported.[17,23] Force constants were computed from a $2 \times 2 \times 2$ supercell expansion, with the k-point sampling reduced accordingly. During post-processing, phonon frequencies and lifetimes were computed on a $16 \times 16 \times 16$ Γ-centered q-point mesh, which was sufficient for convergence of the phonon DOS with our chosen supercell size.

While the thermal physics is determined by the full phonon DOS, IR and Raman spectroscopies probe only the modes at the Brillouin zone centre (Γ point). In Mulliken notation, the irreducible representation of the optical Γ-point modes for kesterite is given as $\Gamma = 3A \oplus 6B \oplus 6E$. Here, the

A and *B* modes are non-degenerate, while the *E* modes are doubly degenerate, resulting in the 21 optical modes expected for the eight-atom primitive cell (i.e., 3*N*-3). According to the selection rules for this crystal symmetry, all modes are Raman active, while only the *B* and *E* modes are IR active. The observable spectra are also weighted by the IR/Raman intensity of the Γ-point modes; the IR intensity is proportional to the square of the dipole induced by the excited phonon, while the Raman intensity is related to the change in polarisability (or, equivalently, the macroscopic high-frequency dielectric constant), along the mode.[25]

The calculated phonon DOS for CZTS is shown in Figure 1(a), while the eigenvectors of the zone-centre modes are illustrated in Figure 2. The lower phonon branch runs from 0 to 175 cm^{-1}, while the higher-energy optic branch runs from 250 to 350 cm^{-1}, in good agreement with previous computational reports.[21,26] The simulated vibrational spectra are shown in Figures 1(b) and 1(c). For CZTS, the strongest IR and Raman modes are measured around 255 cm^{-1} and 336 cm^{-1}, respectively.[24] Both features are in good accord with our predicted spectra; however, the calculated highest frequency band is noticeably softer (i.e. the modes occur at lower vibrational frequency), which can be related to the too-high polarisability of S with gradient-corrected exchange-correlation functionals.[27] Other possible sources of error in the simulations include the use of a structure optimised at 0 K, as well as a periodic crystal with no treatment of defects or disorder. The three *A* modes involve only anion vibrations, relative to fixed cations, whilst the *B* and *E* modes encompass both anion and cation vibrations. The *B* modes involve cation displacements along the *c* direction, while the *E* modes involve in-plane cation vibrations parallel to the *a* direction.

The phonon DOS of CZTSe (Figure 3) has a similar shape to that of CZTS, but is substantially compressed, owing to the larger atomic mass of Se. The crystal symmetry is maintained, and hence, the atomic contributions to the eigenvectors reported in Figure 2 are unchanged. The phonon DOS calculated for CZTSe is in good agreement with previous lattice-dynamics calculations.[28]

Within the harmonic approximation, the phonons in a bulk crystal have an infinite lifetime, due to the absence of scattering events. By considering three-phonon interactions, under the condition of conservation of energy and momentum, phonon lifetimes can be predicted from first principles.[17,23] The spectrum of lifetimes in CZTS and CZTSe is compared in Figure 4. The values range from 1 ps to 1 ns, with the longer lifetimes found at high and low wavenumbers due to fewer scattering events. Interestingly, longer lifetimes are observed for the acoustic modes of the selenide compared to the sulfide, which we attribute to the compressed phonon DOS allowing fewer three-phonon processes.

The lifetimes of the Γ-point phonon modes, obtained from the third-order force constants, have been used to include line broadening in Figure 1. Both Raman and IR absorptions have a Lorentzian lineshape with a full-width at half-maximum (FWHM), Γ, related to the phonon lifetime according to $\tau = \frac{1}{2\Gamma}$. To facilitate better comparison with experimental measurements, the simulated spectra in Figure 1 also include an instrument broadening of 3.5 cm^{-1}, which was added by convoluting the initial simulated spectrum with a second Lorentzian function. With instrument broadening accounted for, the predicted lineshapes of the Raman correspond well with the experimental spectrum.

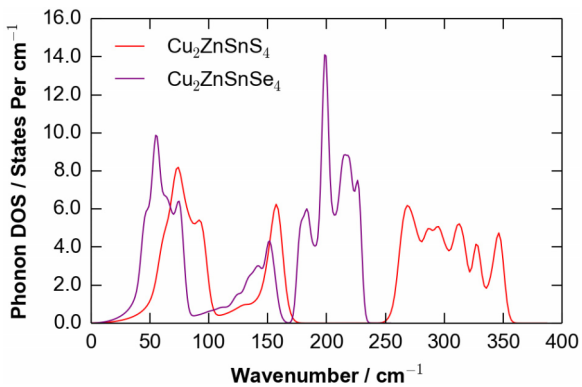

FIG. 3. Comparison of the calculated phonon densities of states of Cu_2ZnSnS_4 and $Cu_2ZnSnSe_4$. Note the lower optic mode frequencies of the selenide compared to the sulfide.

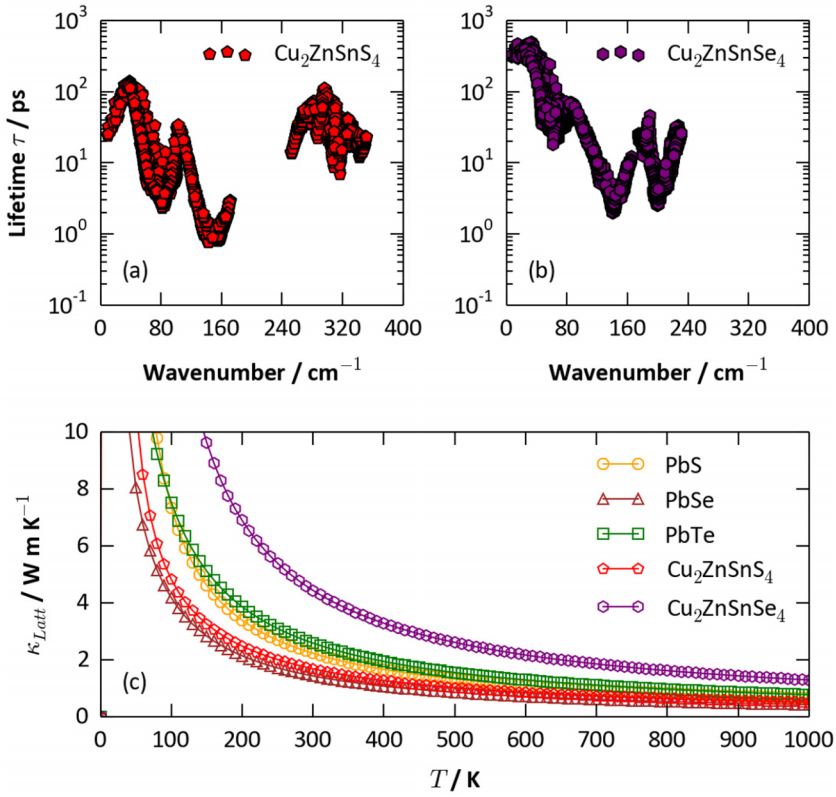

FIG. 4. Computed phonon lifetimes due to three-phonon scattering processes at 300 K in (a) Cu_2ZnSnS_4 and (b) $Cu_2ZnSnSe_4$. (c) Calculated bulk thermal conductivity of Cu_2ZnSnS_4 and $Cu_2ZnSnSe_4$ compared to the lead chalcogenides (data from Ref. 17). The conductivity curves were obtained by solving the Boltzmann transport equation within the relaxation-time approximation.[23]

The temperature-dependent bulk lattice thermal conductivity of CZTS and CZTSe, limited by three-phonon processes, is shown in Figure 4(c). Due to the nature of the Bose-Einstein distribution, it is the low-frequency modes that largely contribute to thermal conductivity and hence the longer mode lifetimes calculated for CZTSe result in a higher conductivity than CZTS. Note that for PbS and PbSe, an opposite trend is observed, as PbS displays the higher conductivity. The isotropically averaged values at ambient temperature (300 K) are 1.69 and 4.44 Wm K^{-1} for CZTS and CZTSe, respectively. The values for CZTS are consistently lower than PbTe and comparable to PbSe. To our knowledge, there have been no reports of the thermal conductivity of bulk crystals of kesterite-structured materials. The measured response of a pellet formed of pressed powders can be influenced by a range of factors—in particular, inter-grain transport. Nonetheless, our predictions are within a factor of 2–3 of the reported conductivity values of CZTS nanodisks (2.95 Wm K^{-1})[29] and powders (4.7 Wm K^{-1})[30] at 300 K.

In summary, we have reported the vibrational properties of kesterite-structured Cu_2ZnSnS_4 and $Cu_2ZnSnSe_4$ from first-principles. General agreement is found with experimental IR and Raman spectra, providing a platform for future investigations concerning defects and disorders. A strong frequency dependence of the phonon lifetimes is found in each material. The bulk lattice thermal conductivity is very low, demonstrating that phonon transport can be suppressed without heavy metals by simply moving to multi-component semiconductors.

We thank A. Togo for discussions on phonon theory and access to Phono3py. We acknowledge membership of the UK's HPC Materials Chemistry Consortium, which is funded by EPSRC Grant No. EP/L000202. J.M.S. is funded by an EPSRC Programme Grant (No. EP/K004956/1). A.J.J. and S.K.W. are funded by the EPSRC Doctoral Training Centre in Sustainable Chemical Technologies (Nos. EP/G03768X/1 and EP/L016354/1). M.D. has received funding from the People Program

(Marie Curie Actions) of the European Union's Seventh Framework Program under REA Grant Agreement No. 316488 (KESTCELLS). A.W. acknowledges support from the Royal Society and the ERC (Grant No. 277757).

[1] B. Shin, O. Gunawan, Y. Zhu, N. A. Bojarczuk, S. J. Chey, and S. Guha, Prog. Photovoltaics **21**, 72 (2013).
[2] W. Wang, M. T. Winkler, O. Gunawan, T. Gokmen, T. K. Todorov, Y. Zhu, and D. B. Mitzi, Adv. Energy Mater. **4**, 1301465 (2014).
[3] T. Gokmen, O. Gunawan, and D. B. Mitzi, Appl. Phys. Lett. **105**, 033903 (2014).
[4] O. Gunawan, T. Gokmen, and D. B. Mitzi, J. Appl. Phys. **116**, 084504 (2014).
[5] S. Chen, X. G. Gong, A. Walsh, and S.-H. Wei, Phys. Rev. B **79**, 165211 (2009).
[6] S. Chen, X. G. Gong, A. Walsh, and S.-H. Wei, Appl. Phys. Lett. **94**, 041903 (2009).
[7] J. J. S. Scragg, L. Choubrac, A. Lafond, T. Ericson, and C. Platzer-Björkman, Appl. Phys. Lett. **104**, 041911 (2014).
[8] F. Espinosa-Faller, J. Phys. Chem. C **118**, 26292 (2014).
[9] G. Rey, A. Redinger, J. Sendler, T. P. Weiss, M. Thevenin, M. Guennou, B. El Adib, and S. Siebentritt, Appl. Phys. Lett. **105**, 112106 (2014).
[10] Y. T. Zhai, S. Y. Chen, J. H. Yang, H. J. Xiang, X. G. Gong, A. Walsh, J. Kang, and S. H. Wei, Phys. Rev. B **84**, 075213 (2011).
[11] P. Fernandes, P. Salomé, and A. Da Cunha, Thin Solid Films **517**, 2519 (2009).
[12] X. Fontané, L. Calvo-Barrio, V. Izquierdo-Roca, E. Saucedo, A. Pérez-Rodriguez, J. Morante, D. Berg, P. Dale, and S. Siebentritt, Appl. Phys. Lett. **98**, 181905 (2011).
[13] J. J. Scragg, J. T. Watjen, M. Edoff, T. Ericson, T. Kubart, and C. Platzer-Bjrkman, J. Am. Chem. Soc. **134**, 19330 (2012).
[14] M. Dimitrievska, A. Fairbrother, X. Fontané, T. Jawhari, V. Izquierdo-Roca, E. Saucedo, and A. Pérez-Rodríguez, Appl. Phys. Lett. **104**, 021901 (2014).
[15] M. Dimitrievska, A. Fairbrother, A. Pérez-Rodríguez, E. Saucedo, and V. Izquierdo-Roca, Acta Mater. **70**, 272 (2014).
[16] J. P. Perdew, A. Ruzsinszky, G. I. Csonka, O. A. Vydrov, G. E. Scuseria, L. A. Constantin, X. Zhou, and K. Burke, Phys. Rev. Lett. **100**, 136406 (2008).
[17] J. M. Skelton, S. C. Parker, A. Togo, I. Tanaka, and A. Walsh, Phys. Rev. B **89**, 205203 (2014).
[18] G. Kresse and J. Furthmüller, Phys. Rev. B **54**, 11169 (1996).
[19] G. Kresse and J. Furthmüller, Comput. Mater. Sci. **6**, 15 (1996).
[20] P. E. Blöchl, Phys. Rev. B **50**, 17953 (1994).
[21] A. J. Jackson and A. Walsh, J. Mater. Chem. A **2**, 7829 (2014).
[22] A. Togo, L. Chaput, I. Tanaka, and G. Hug, Phys. Rev. B **81**, 174301 (2010).
[23] A. Togo, L. Chaput, and I. Tanaka, Phys. Rev. B **91**, 094306 (2015).
[24] M. Himmrich and H. Haeuseler, Spectrochim. Acta, Part A **47**, 933 (1991).
[25] D. Porezag and M. Pederson, Phys. Rev. B **54**, 7830 (1996).
[26] A. Khare, B. Himmetoglu, M. Johnson, D. J. Norris, M. Cococcioni, and E. S. Aydil, J. Appl. Phys. **111**, 083707 (2012).
[27] C. Van Caillie and R. D. Amos, Chem. Phys. Lett. **328**, 446 (2000).
[28] N. B. Mortazavi Amiri and A. Postnikov, Phys. Rev. B **82**, 205204 (2010).
[29] H. Yang, L. A. Jauregui, G. Zhang, Y. P. Chen, and Y. Wu, Nano Lett. **12**, 540 (2012).
[30] M.-L. Liu, F.-Q. Huang, L.-D. Chen, and I.-W. Chen, Appl. Phys. Lett. **94**, 202103 (2009).